

Mitochondria Provide the Main Source of Cytosolic ATP for Activation of Outward-rectifying K⁺ Channels in Mesophyll Protoplast of Chlorophyll-deficient Mutant Rice (*OsCHLH*) Seedlings*

Received for publication, August 15, 2003, and in revised form, December 2, 2003
Published, JBC Papers in Press, December 3, 2003, DOI 10.1074/jbc.M309071200

Chang-Hyo Goh^{‡§}, Ki-Hong Jung[¶], Stephen K. Roberts^{||}, Martin R. McAinsh^{||},
Alistair M. Hetherington^{||}, Youn-il Park^{**}, KyeHong Suh^{‡‡}, Gynheung An[¶], and Hong Gil Nam[¶]

From the [‡]Bionanotechnology Center, Department of Life Science, Pohang University of Science and Technology, the [¶]Division of Molecular and Life Science, Pohang University of Science and Technology, Kyungbuk 790-784, Korea, the ^{||}Department of Biological Sciences, University of Lancaster, Lancaster LA1 4YQ, United Kingdom, the ^{**}Department of Biology, Chungnam National University, Taejon 305-764, Korea, and the ^{‡‡}Division of Life Science, Daegu University, Daegu 712-714, Korea

The role of mitochondria in providing intracellular ATP that controls the activity of plasma membrane outward-rectifying K⁺ channels was evaluated. The *OsCHLH* rice mutant, which lacks chlorophyll in the thylakoids, was isolated by T-DNA gene trapping (Jung, K.-H., Hur, J., Ryu, C.-H., Choi, Y., Chung, Y.-Y., Miyao, A., Hirochika, H., and An, G. (2003) *Plant Cell Physiol.* 44, 463–472). The *OsCHLH* mutant is unable to fix CO₂ and exhibits reduced growth. Wild type and mutant plants exhibit similar rates of respiratory O₂ uptake in the dark, whereas the rate of photosynthetic O₂ evolution by the mutant was negligible during illumination. During dark respiration the wild type and mutant exhibited similar levels of cytoplasmic ATP. In the mutant oligomycin treatment (an inhibitor of mitochondrial F₁F₀-ATPase) drastically reduced ATP production. The fact that this was reversed by the addition of glucose suggested that the mutant produced ATP exclusively from mitochondria but not from chloroplasts. In whole cell patch clamp experiments, the activity of outward-rectifying K⁺ channels of rice mesophyll cells showed ATP-dependent currents, which were 1.5-fold greater in wild type than in mutant cells. Channels in both wild type and mutant cells were deactivated by the removal of cytosolic ATP, whereas in the presence of ATP the channels remained active. We conclude that mesophyll cells in the *OsCHLH* rice mutant derive ATP from mitochondrial respiration, and that this is critical for the normal function of plasma membrane outward-rectifying K⁺ channels.

Mitochondrial metabolism not only impacts on other cellular biosynthetic and catabolic processes, but also plays an important role in providing the overall cellular energy supply. Dark respiration and photosynthesis are metabolic pathways that produce redox equivalents and ATP to meet the energy requirements to support cell growth and maintenance (2). The central

role of mitochondria in plants is reflected by the array of mitochondrial transporters and shuttles that transfer metabolites and reducing equivalents back and forth between mitochondria and the cytosol. Oxidative phosphorylation provides the cytosol with ATP, which is required for sucrose synthesis and other cytosolic processes. Studies with specific respiratory inhibitors have shown that oxidative phosphorylation occurs both in darkness and in light (2–4). However, very little is known about the regulation of mitochondrial respiration in photosynthetic mesophyll cells, and the role of mitochondrial ATP production as a source of cytosolic ATP in this process is not fully understood.

Many biochemical reactions in plant and mammalian cells depend on a tightly controlled ratio of ATP to ADP. In mammalian mitochondria, this ratio is preserved by regulatory mechanisms that couple the rate of cellular ATP consumption to the rate of ATP production by oxidative phosphorylation (5–8). Hence, efficient communication between cellular energy stores and membrane metabolic sensors is necessary for regulation of membrane excitability and associated functions. In most mammalian cells, there is a class of K⁺ channels whose activity is closely coupled to metabolism by ATP (9, 10). Recent studies have shown that oxidative phosphorylation, through its effect on ATP synthesis, plays an essential role in the regulation of ATP-sensitive K⁺ channels (11–13). However, it has also been reported that glycolytic ATP preferentially controls these channels (11, 14, 15).

In plant mesophyll cells, outward-rectifying K⁺ (K_{out})¹ channels activated by membrane depolarization serve as the primary pathway for K⁺ efflux. As K_{out} channel activity is completely abolished (within 15 min) in the absence of cytosolic ATP (16–19), it can be concluded that K⁺ efflux in plant cells is ATP-dependent. However, the roles of photophosphorylation and oxidative phosphorylation in the regulation of K_{out} channels remain controversial. Light activates the H⁺ pump current (20–23), K⁺ channels (16, 24–26), and regulates membrane potential (27–29) in photosynthetic cells, suggesting that these cells are sensitive to some aspects of metabolic energy within the cytosol. Light-induced activation of the H⁺ pump in mesophyll cells may require both photosynthetic products (*i.e.*

* This work was supported by a Korea and United Kingdom scientist exchange program (to C.-H. G.) and partly supported by Brain Korea 21 and Korean Research Foundation Grant 2003-005-C00011. The costs of publication of this article were defrayed in part by the payment of page charges. This article must therefore be hereby marked "advertisement" in accordance with 18 U.S.C. Section 1734 solely to indicate this fact.

§ To whom correspondence should be addressed. Tel.: 82-54-279-8283; Fax: 82-54-279-2199; E-mail: gohunse@postech.ac.kr.

¹ The abbreviations used are: K_{out}, outward-rectifying K⁺; Mes, 2-(N-morpholino)ethanesulfonic acid; PS II, photosystem II; DCMU, dichlorophenyl dimethylurea.

sugars) and a non-photosynthetic light effect (20, 28). On the other hand, the light-modulated transport system in mesophyll cells induced a rapid depolarization, which was immediately followed by repolarization and a subsequent slower hyperpolarization (16, 27–31). The hyperpolarization seemed to be regulated by changes in activity of the plasma membrane H^+ -ATPase and voltage-dependent ion channels (31–33). Analysis of metabolites in the presence of oligomycin, which blocked the F_1F_0 -ATPase, revealed a dramatic decrease in the mitochondrial and cytosolic ATP concentration (34), indicating that mitochondria-driven ATP production was decreased. Whereas some reports suggest that the activation of K_{out} channels and membrane potential in mesophyll cells is regulated by ATP derived from photosynthesis (16, 29), a more recent study shows that leaf mitochondria modulate whole cell redox homeostasis (35). These conflicting findings prompted us to evaluate the effects of ATP on the K_{out} channels in mutant, chlorophyll-deficient rice cells.

To explore this in mesophyll cells, we exploited a chlorophyll-deficient rice mutant (*OsCHLH*), which lacks the largest subunit of Mg^{2+} -chelatase (1). This rice mutant is defective in photoperception, and was therefore useful for investigating the source of cytosolic ATP that controls K_{out} channels. Here we show that the activity of K_{out} channel in chlorophyll-deficient mutant cells is controlled by a cytosolic pool of ATP that is predominantly derived from oxidative phosphorylation. Cytosolic ATP production was further enhanced by the addition of glucose. These results strongly suggest that there is metabolic cross-talk between mitochondria and K_{out} channel activity in rice chlorophyll-deficient mesophyll cells.

MATERIALS AND METHODS

Plant Material—Seedlings were grown and mutants screened on media containing 0.44% Murashige and Skoog basal salt, 3% sucrose, 0.2% phytigel, and 0.55 mM *myo*-inositol (Sigma) for 8 days unless otherwise stated. The plants (*Oryza sativa* cv. Japonica) were cultured in a temperature-controlled growth chamber at $28 \pm 1^\circ C$ under a 16-h day cycle, at a minimum photon flux density of $90 \mu mol m^{-2} s^{-1}$.

Chlorophyll Fluorescence Imaging—Leaf tissue was harvested from 8-day-old seedlings. Mesophyll protoplasts were prepared as previously described (36). The fluorescence signal was monitored using a fluorescent microscope (Axioplan 2, Zeiss, Jena, Germany). Images were processed using an automatic imaging system (FISH, Carl Zeiss).

Inverse PCR—Inverse PCR methodology was described previously (1). The PCR product was directly subjected to sequencing reactions using the primer 5'-GCAAGGATACAAGTCTGTACCT-3'.

Measurements of Net CO_2 Uptake by Leaf Gas Exchange—Rates of net CO_2 uptake by attached leaves were measured in an open gas exchange system (LCA2, ADC, Hoddesdon, UK) coupled to a mass spectrometer as described previously (37). Air entering the Parkinson leaf chamber was conditioned at 40% relative humidity, 370–380 $\mu l liter^{-1} CO_2$, at a flow rate of 200 ml min^{-1} . Leaf temperature in the chamber was maintained at $25^\circ C$ with a temperature controller (Prime Bio Chemical Co., Seoul, Korea). Incident photon flux densities were supplied by a fiber optic illuminator (Schott, Mainz, Germany) from a halogen lamp (20 W, Phillips, Eindhoven, Netherlands) and measured with a silicon photodiode detector (MMS, Zeiss). Neutral density filters were used to vary light intensity.

Determination of Net O_2 Evolution and Net O_2 Uptake—Leaf discs were excised and introduced into a leaf disc O_2 electrode chamber (Hansatech Instruments, King's Lynn, Norfolk, UK) in a closed gas exchange system of air with 5% CO_2 at $26 \pm 2^\circ C$ as described previously (38). After calibration, the steady-state rate of O_2 consumption was monitored until a stable rate was reached. Leaf discs were then illuminated at an irradiance of 60 and 900 $\mu mol m^{-2} s^{-1}$. Rates of net O_2 evolution and net O_2 uptake were determined as described by Walker (39). The actinic light was provided by a 150-W quartz-halogen slide projector fitted with heat filters through neutral density filters.

Analysis of Total Cellular ATP Levels—The amount of ATP was measured by the luciferin-luciferase method (40) in intact seedlings (Fig. 4A) and isolated mesophyll protoplasts (Fig. 4B). The *OsCHLH* rice mutants were harvested about 2 h into the dark and light ($90 \mu mol m^{-2} s^{-1}$) periods, respectively, and stored in liquid nitrogen until anal-

ysis. The leaves were extracted and analyzed on the day they were sampled. The protoplasts were incubated in a temperature-controlled room ($28 \pm 1^\circ C$) for 40 min in the dark. The protoplasts (30 $\mu g/ml$) were incubated in incubation medium (0.6 M sorbitol, 1 mM $CaCl_2$, 10 mM KCl, 10 mM Mes-NaOH (pH 6.2)) with various combinations of substrate and inhibitors. ATP was extracted from 100 μl of cell suspension by adding 2.5% trichloroacetic acid using an ENLITEN ATP assay bioluminescence detection kit (Promega, Madison, WI), according to the manufacturer's recommended protocol. The extracted ATP solution was neutralized by 0.75 M Tris acetate buffer (pH 7.75) and centrifuged for 10 min at $1,600 \times g$. The resulting supernatant was used in ATP determination assays. The reaction was initiated by adding 100 μl of the extract to 100 μl of the luciferin-luciferase luminous reagent (Promega). The luminescence was integrated for 5 s using a luminometer (Luminoskan Ascent 2.1 Int., Turuku, Finland). The actual ATP levels were calculated from an ATP standard curve constructed using commercially supplied ATP.

Whole Cell Patch Clamp Recording—Before use in the patch clamp experiments, mesophyll cell protoplasts were kept in a solution including 1 mM $CaCl_2$ adjusted with D-sorbitol to 600 mmol kg^{-1} . The dimensions of the protoplasts were fairly consistent, with diameters of $16.6 \pm 0.43 \mu m$ for the wild type and $15.1 \pm 0.35 \mu m$ for the mutant. Whole cell recording was performed as described by Li and Assmann (42). Briefly, the standard patch pipette solution contained (in mM) 100 K-glutamate, 2 EGTA, 2 $MgCl_2$, 2 KCl, and 10 Hepes with or without 2 MgATP, titrated to pH 7.2 with Tris. The bath solution consisted of 10 mM K-glutamate, 1 mM $CaCl_2$, 4 mM $MgCl_2$, and 10 mM HEPES titrated to pH 7.2 with Tris. Osmolalities were adjusted with D-sorbitol to 696 mmol kg^{-1} for the pipette solution and 623 mmol kg^{-1} for the bath solution. During whole cell recordings, the membrane potential was held at -40 mV, except during voltage steps. Currents across the membrane were measured upon imposition of a series of voltage pulses from -160 to $+100$ mV with 20-mV increments, as described previously (42). Liquid junction potential was measured and corrected (43). Seal resistances were in the range of 1.5 to 4 gighohm. For whole cell experiments, application of voltage programs and handling of the data were performed using a Digidata 1200 interface and patch clamp software pClamp8.0 with Calmpex and Clampfit (Axon instruments). Whole cell data were low-pass filtered with an eight-pole Bessel filter at a cut-off frequency of 2 kHz. Capacitance and pipette offset potentials were compensated during the patch clamp experiments.

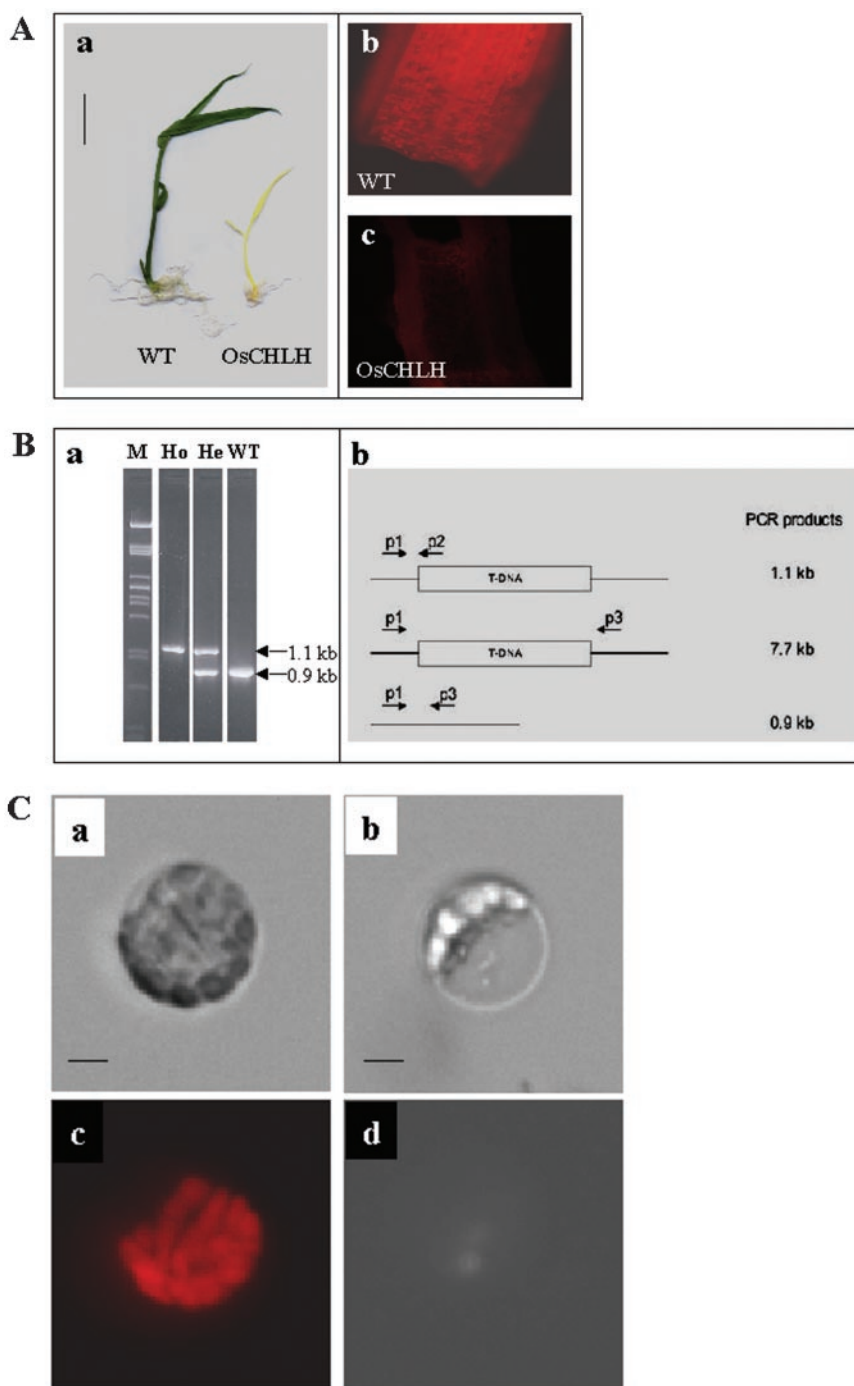
Data Analysis—Group data are expressed as mean \pm S.E. Comparisons among groups were made by analysis of variance (F-test). Bonferroni-adjusted *t* tests were used for multiple group comparisons and paired or unpaired *t* tests were used, as appropriate, for single comparisons. Nonlinear least-square curve fitting was performed with CLAMPFIT in pCLAMP 8.0.

RESULTS

The *OsCHLH* Mutation Affects Chlorophyll Pigmentation of the Rice Seedlings—To study the mitochondrial contribution to the cytosolic ATP pool in photosynthetic cells, we used the chlorophyll-deficient *OsCHLH* rice mutant (Fig. 1A). We previously identified this mutant as a knockout of *OsCHLH*, the gene encoding Mg^{2+} -chelatase that is involved in chlorophyll biosynthesis (1). The *OsCHLH* mutant contains only 0.27% or less of the normal chlorophyll content (on a per leaf area basis) (1) and did not exhibit chlorophyll fluorescence in its intact leaves (Fig. 1A, panel c) or in mesophyll cells (Fig. 1C, panel d). This chlorina phenotype co-segregated with a T-DNA insertion in which the *OsCHLH* mutation was a single recessive mutation (1). The vector used for mutagenesis carried the promoterless β -glucuronidase reporter gene immediately adjacent to the 3' border of T-DNA. The T-DNA-tagged lines could be therefore verified by β -glucuronidase assay (data not shown). This mutant carries a stable DNA mutation that affects chlorophyll synthesis in the thylakoid light-harvesting complexes (1, 44).

The growth of *OsCHLH* mutant seedlings was comparable with the wild type (Fig. 1A, panel a). The fresh weight of 8-day-old seedlings was 0.061 ± 0.011 and 0.031 ± 0.008 g for wild type and *OsCHLH* mutant plants, respectively. The addition of sucrose, which stimulates ATP generation by respiration (36), enhanced the growth in both wild type and mutant plants, showing 33.3 and 52.9% increases for the wild type and

FIG. 1. Phenotype and genotype of *OsCHLH* rice plants. *A*, whole 8-day-old seedlings of wild type (*a*, left) and *OsCHLH* mutant plants (*a*, right). The *OsCHLH* mutant lacks chlorophyll in the leaves of the seedlings. *Panel b* shows chlorophyll fluorescence in a representative wild type leaf and *panel c* shows chlorophyll fluorescence in an *OsCHLH* mutant leaf of 8-day-old seedlings. The bar indicates 1.6 cm. *B*: *a*, genomic DNA from T2 plants was subjected to PCR analysis with the primers shown in *panel C*. Only the 1.1-kb fragment, the 0.9-kb fragment, or both fragments were amplified by PCR in homozygous (*Ho*), wild type (*WT*), and *OsCHLH* heterozygous (*He*) T3 plants, respectively. *M* indicates the λ DNA size marker cut with PstI. *b*, schematic representation of the gene structures in the region that complemented the *OsCHLH* mutant phenotype. *p1*, forward primer in *OsCHLH*; *p2*, reverse primer in T-DNA; *p3*, reverse primer in *OsCHLH*. The *p1* and *p2* primers amplified the 1.1-kb PCR product from the T-DNA inserted DNA template. The *p1* and *p3* primers produced the 0.9-kb PCR product from the DNA of wild type plants. In contrast, no PCR band was obtained from the T-DNA inserted template, because the predicted fragment size (7.7 kb) was too large to amplify (1). *C*, chlorophyll fluorescence of homozygous *OsCHLH* rice mesophyll cells isolated from the leaves of 8-day-old seedlings. *a* and *b*, light micrograph of wild type and *OsCHLH* mutant protoplasts. *c* and *d* show the red chlorophyll fluorescence from the same field of the cells of *a* and *b*, respectively. Mesophyll cells were suspended in a solution including 1 mM $CaCl_2$ adjusted with D-sorbitol to 600 mmol kg^{-1} . The bars indicate 5 μm .



OsCHLH mutant plants, respectively (data not shown). Although the mutants did not live longer than 4–5 weeks, these data indicate that mitochondria can contribute to the cellular energy requirements of the *OsCHLH* mutants.

Photosynthetic CO_2 Uptake—The photosynthetic capacity of the *OsCHLH* mutant was studied in intact plants by CO_2 gas exchange (Fig. 2A). Whereas in the wild type there was significant CO_2 uptake in the light, there was no CO_2 uptake in the *OsCHLH* mutant plants. The *OsCHLH* mutant plants also released more CO_2 than the wild type during dark respiration (Fig. 2B). Although it showed a substantial decrease, CO_2 release was observed in the *OsCHLH* mutant even under saturating light conditions. On the basis of chlorophyll concentration of this mutant, the decrease in CO_2 release appears to be because of the inhibition of mitochondrial respiration by light.

This result implies that the *OsCHLH* mutant plants have no CO_2 fixation capacity.

Respiratory O_2 Uptake and Photosynthetic O_2 Evolution—In light, transients in chlorophyll fluorescence and oxygen evolution reflect mechanisms regulating CO_2 assimilation (36, 45, 46). The transients might be related to regulatory mechanisms involving, particularly, the cytosolic [ATP]/[ADP] ratio that favors electron transport (26). We need therefore to investigate the activity of O_2 -evolving photosystem II (PS II) in the mutant chloroplasts. In preliminary experiments, CP43 immunoreactivity was readily detected in isolated thylakoid membranes from wild type, but not in *OsCHLH* mutant seedlings (data not shown), suggesting that PS II activity is impaired in the *OsCHLH* mutant. We then measured oxygen evolution as a function of light intensity in leaf discs (Fig. 3). The voltage

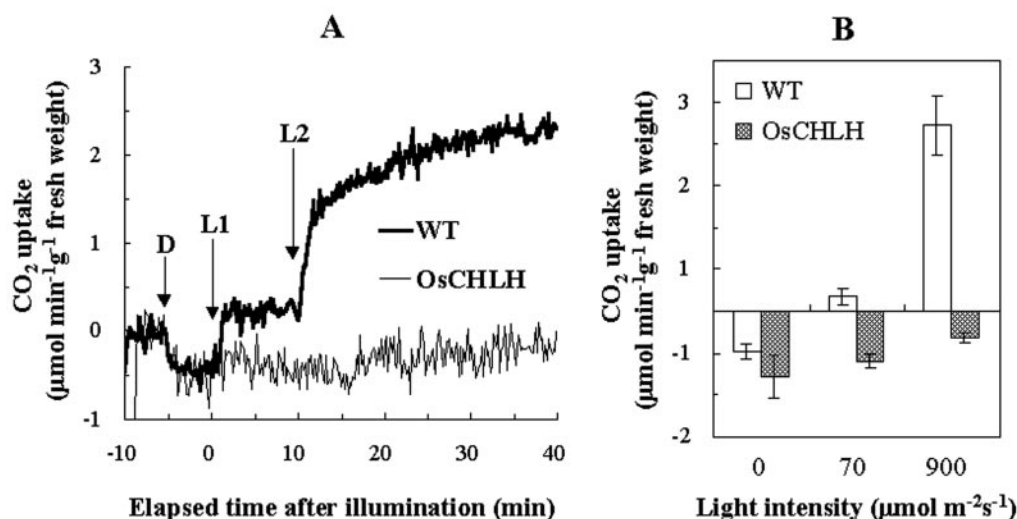


FIG. 2. Changes of CO_2 exchange rates in intact leaves of wild type and homozygous *OsCHLH* mutant plants. A, typical recordings of CO_2 exchange during dark-light transitions measured by leaf gas exchange. Attached leaves from 2-week-old seedlings of two wild type or *OsCHLH* mutant plants were first adapted to dark (D) for 5 min. Light was turned on when indicated by the vertical arrows (L1, $70 \mu\text{mol m}^{-2} \text{s}^{-1}$ for 10 min; and L2, $900 \mu\text{mol m}^{-2} \text{s}^{-1}$ for 30 min). Bold and fine lines indicate CO_2 exchange in wild type (WT) and mutant (*OsCHLH*) leaves, respectively. B, histograms show net CO_2 uptake in the dark (0) and under 70 and $900 \mu\text{mol m}^{-2} \text{s}^{-1}$ actinic light, as indicated. Data are expressed as mean \pm S.E. from three separate experiments. The differences between the means were statistically significant (*t* test, $p = 0.05$), except for dark experiments (*t* test, $p = 0.144$). Other experimental conditions were described under "Materials and Methods."

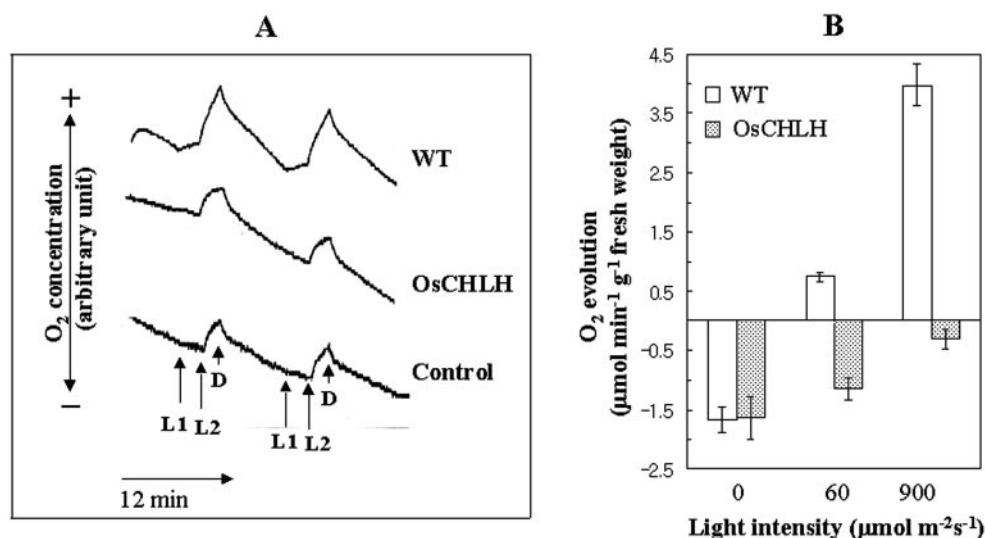


FIG. 3. Oxygen evolution and consumption in detached leaves of wild type and homozygous *OsCHLH* mutant plants. A, the time course of a typical experiment showing the output voltage from an oxygen sensor (logged twice every second). The scaling is linear. Four leaf discs were provided with bicarbonate as a source of carbon dioxide and kept in the dark for 9 min prior to the start of logging and then illuminated. On the vertical (oxygen concentration) axis, + and - indicate net oxygen production and net oxygen consumption, respectively. L1 and L2 indicate applications of actinic light at 60 and $900 \mu\text{mol m}^{-2} \text{s}^{-1}$, respectively, whereas D represents dark treatment. A blank (without leaf material) was included as control (bottom) and its signal (L2) was increased artificially by increasing light intensity ($900 \mu\text{mol m}^{-2} \text{s}^{-1}$), inducing an increase in temperature. B, histograms show net oxygen consumption in the dark (0) and net oxygen evolution under 60 and $900 \mu\text{mol m}^{-2} \text{s}^{-1}$ actinic light, as indicated. Data are expressed as mean \pm S.E. from five separate experiments. The differences between the means were statistically significant (*t* test, $p = 0.05$), except for dark experiments. Net oxygen concentrations were measured over the final 2-min period of the dark and actinic light intervals. Data subtracted from control values and log transformed, such that the gradient of a fitted line, using regression analysis, would constitute the exponential decay constant (*k*) of the form $R_t = R_0 \times e^{-kt}$ (39), where R_t is the respiration rate at the start of the dark period and R_0 is the respiration rate at some time, *t*. Other experimental conditions were described under "Materials and Methods."

output from the oxygen sensor from a typical trial is shown in Fig. 3A. Each leaf was placed in darkness for 9 min, and then exposed to actinic light (L1 and L2) for 3 min. This was followed by another 6-min period of darkness. In wild type, the photosynthetic O_2 evolution increased from 0.71 to $3.98 \mu\text{mol min}^{-1} \text{g}^{-1}$ fresh weight, depending on light intensity (Fig. 3B). There was, however, no photosynthetic O_2 evolution in the mutant. In addition, mitochondrial respiration in the mutant was regulated by light, in that the rates of oxygen uptake were decreased from 1.5 to $0.3 \mu\text{mol min}^{-1} \text{g}^{-1}$ fresh weight with light treatment, suggesting that light inhibited mitochondrial respi-

ration in the mutant (for review see Refs. 2 and 34). In the dark, there were no statistically significant differences in O_2 evolution between wild type and mutant leaves (*t* test, $\alpha = 0.042$). Taken together, these data indicate that the *OsCHLH* mutant seedlings exhibited high levels of mitochondrial respiration similar to wild type, but completely lacked the capacity to perform photosynthesis.

ATP Content in Wild Type and *OsCHLH* Mutant Mesophyll Cells—Because total cellular ATP levels are directly associated with respiratory O_2 uptake and ATP synthesis in mitochondria in darkness (47), we next measured total cellular ATP levels. In

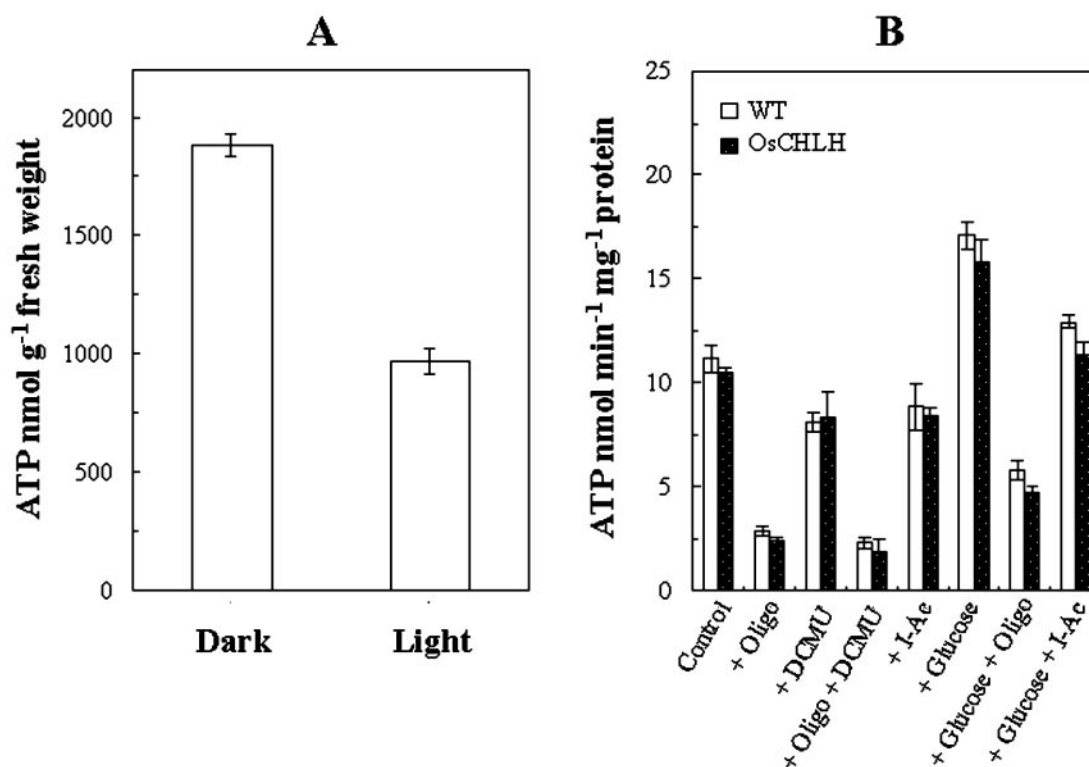


FIG. 4. ATP content in intact seedlings and mesophyll protoplasts of homozygous *OsCHLH* mutant plants. A, the mutant seedlings were grown for 8 days in a 16-h day cycle, at a minimum photon flux density of $90 \mu\text{mol m}^{-2} \text{s}^{-1}$ and then harvested 2 h after dark and light ($90 \mu\text{mol m}^{-2} \text{s}^{-1}$) treatments, respectively. ATP production was determined as described under "Materials and Methods." Data are expressed as mean \pm S.E. ($n = 6$). The differences between the means were statistically significant (t test, $p < 0.001$). B, cells were incubated with various combinations of substrate (glucose, 5 mM), oligomycin (*Oligo*, $2 \mu\text{g ml}^{-1}$), DCMU (10 μM), and iodoacetic acid (*I-Ac*, 1 mM) for 40 min under darkness. Glucose was included as a mitochondrial substrate via glycolysis. Oligomycin and DCMU were used to block mitochondrial F_1F_0 -ATPase and photosynthetic electron transport, respectively. Iodoacetic acid was used to block glycolysis. Data are expressed as mean \pm S.E. ($n = 3$). The differences between the means were statistically significant (t test, $p = 0.05$). The amount of protein was determined by the method of Bradford (41) using BSA as a standard.

dark-treated mutant seedlings the ATP level was 1.88, whereas in the light it was $0.97 \mu\text{mol of ATP g}^{-1}$ fresh weight (Fig. 4A). ATP production was significantly (51.4%) inhibited in the light. This result supported the close association between ATP synthesis and respiratory O_2 uptake as shown in Fig. 3B. Fig. 4B shows the ATP content in wild type and mutant mitochondria of mesophyll cell protoplasts in the dark. Cells were incubated in darkness for 40 min in the presence or absence of 5 mM glucose, which stimulates the generation of ATP by respiration, with various combinations of metabolic inhibitors. As expected, cytosolic ATP levels were quite similar in wild type and mutant cells under control conditions ($\sim 10 \text{ nmol min}^{-1} \text{ mg}^{-1}$ protein). When the F_1F_0 -ATPase was blocked by the respiratory inhibitor, oligomycin ($2 \mu\text{g ml}^{-1}$), ATP production was decreased by a similar level (74 and 77%), in wild type and mutant cells, respectively. The respiration activity indicates that the *OsCHLH* mutant cells have levels of mitochondrial oxidative phosphorylation similar to that of the wild type. ATP content was decreased by treatment with 10 μM dichlorophenyl dimethylurea (DCMU) an inhibitor of photosynthetic electron transport. This is probably because of a secondary effect of DCMU on mitochondrial function (48). The combination of oligomycin and DCMU significantly inhibited ATP production in both mutant and wild type cells showing that oligomycin is effective in both types of cell. When glycolysis was blocked by the addition of 1 mM iodoacetic acid to a substrate-free bath solution, cytosolic ATP content was decreased by $\sim 20\%$ in both mutant and wild type cells, indicating that glycolysis produced a relatively small amount of ATP. In the presence of glucose in the bath solution, ATP levels were increased by $\sim 50\%$ in both

wild type and mutant cells. This effect of glucose was largely decreased when oligomycin was included with glucose in the bath solution (oligomycin decreased ATP production by $\sim 66\%$ in wild type and 71% in the mutant cells). Iodoacetic acid inhibited the production of ATP by $\sim 25\%$ in both cell types, relative to the effects of glucose alone. This implies that glycolysis in the mutant cells proceeds at similar rates to that found in the wild type. Taken together, these findings suggest that the cytosolic ATP pool was predominantly produced by mitochondrial oxidative phosphorylation in the mutant.

Voltage- and Time-dependent ATP-sensitive K_{out} Channels—To test the voltage and time dependence of membrane currents, a series of voltage pulses was applied to the plasma membrane in the whole cell configuration. Typical whole cell current time courses in the presence or absence of ATP are shown in Fig. 5. The whole cell patch clamp recordings showed that rice mesophyll cells lacked the inward-rectifying K^+ channel activity described in tobacco (49), oat (50), and *Vicia* mesophyll cells (42). These mesophyll cells display a similar pattern of K^+ currents as a yeast mutant (*Trk1 Δ Trk2 Δ*) (52). The following experiments demonstrated that ATP was required for the activation of K_{out} channels of both wild type and mutant mesophyll cells, similar to what has been reported previously (17–19, 42, 49, 50). The addition of 2 mM ATP to the cytoplasmic side of protoplasts stimulated voltage-dependent K_{out} channels in both wild type and mutant cells (Fig. 5, B and C, left panels). In whole cell measurements in the absence of ATP, 8-min run-down effects of the outward current were observed in both cell types (Fig. 5, B and C, right panels). The effect of ATP was statistically significant at positive membrane poten-

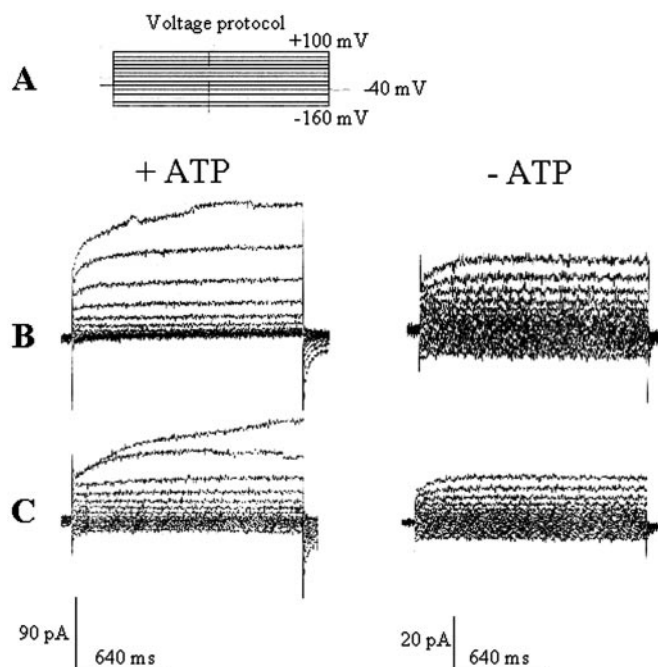


FIG. 5. Whole cell currents in mesophyll protoplasts of wild type and homozygous *OsCHLH* mutant plants. A, voltage protocol for all whole cell measurements. Representative current measurements in wild type cells (B) and mutant *OsCHLH* (C) cells are shown. +ATP and -ATP indicate the presence and absence of ATP in the pipette solution, respectively. Currents were measured after 8 min of perfusion in either the presence (left panels of B and C) or absence (right panels of B and C) of 2 mM ATP in the pipette solution. The holding potential was set at -40 mV, and voltage steps were increased by 20-mV increments from -160 to +100 mV. The right panels of B and C show the current traces at 4.5 scales for easier visualization of kinetics. The stimulation of the K_{out} channel current by intracellularly administered ATP as induced by the voltage steps is shown in A. Left panels show a K_{out} channel current when 2 mM ATP (Tris salt) was perfused into the cell interior with the patch pipette solution. Seal resistance, $R_s = 2.83$ gigaohm; whole cell capacitance, $C = 10.12$ pF (upper trace), $r = 2.70$ gigaohm; $C = 10.18$ pF (lower trace). Right panels show a K_{out} channel current in the absence of ATP (control). $r = 2.07$ gigaohm; $C = 9.78$ pF (upper trace), $r = 2.18$ gigaohm; $C = 10.06$ pF (lower trace). The average cell diameters were 15.7 and 15.2 μm for wild type and mutant cells, respectively.

tials in both wild type and mutant cells (Fig. 6). In the absence of ATP, whole cell currents were run down in similar rates in both cells; they showed about 78–80% inhibition at +100 mV as compared in those of +ATP conditions in both cells, respectively. The run-down effect of K_{out} channel activity could be prevented in both cell types by the addition of 2 mM ATP, although the magnitude of the channel current was smaller in mutant cells. It is possible that the number of K^+ channels in the plasma membrane is greater in wild type cells than in the mutant. The modulation of channel density is regarded as an important mechanism for controlling the transport rate across the plasma membrane in an increasing number of systems (53). This might bring about reduced growth in the mutant seedlings compared with the wild type (Fig. 1A) and therefore result in the reduced size of protoplasts (compare wild type, 16.6 ± 0.43 μm with mutant 15.1 ± 0.35 μm) (Fig. 1C). This ATP dependence of the K_{out} channel is similar to that observed in a variety of cell types and plant species (17–19, 54–58).

Analysis of K_{out} Channels Activated by Membrane Depolarization in *OsCHLH* Rice Mutant Cells—The activity of ATP-dependent K^+ efflux in plasma membranes was maintained in the presence of ATP in the cytosolic solution for 10 min in both wild type (Fig. 7A) and mutant cells (Fig. 7B). When cytosolic ATP was depleted using an ATP-free pipette solution, K_{out}

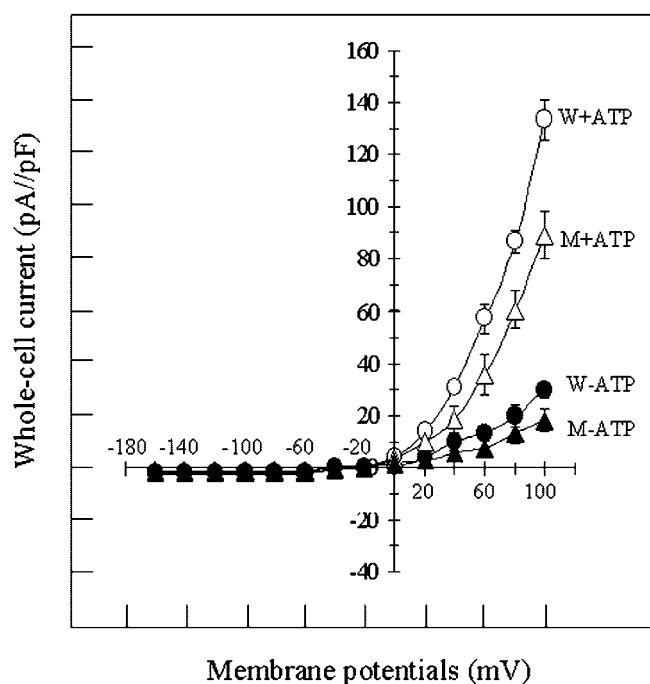


FIG. 6. Current-voltage (I-V) relationship of whole cell currents in mesophyll protoplasts of wild type and homozygous *OsCHLH* mutant seedlings. Recordings were made after perfusing the cells for 8 min in the presence (+ATP, open symbols) or absence (-ATP, closed symbols) of 2 mM ATP in the pipette solution, as indicated. Data are derived from currents shown in Fig. 5 and are presented as the average \pm S.E. ($n = 9$). The voltage steps ranged between -160 and +100 mV in 20-mV increments from a holding potential of -40 mV. W, wild type (circles); M, mutant (triangles). Other experimental conditions are as described in the legend to Fig. 5.

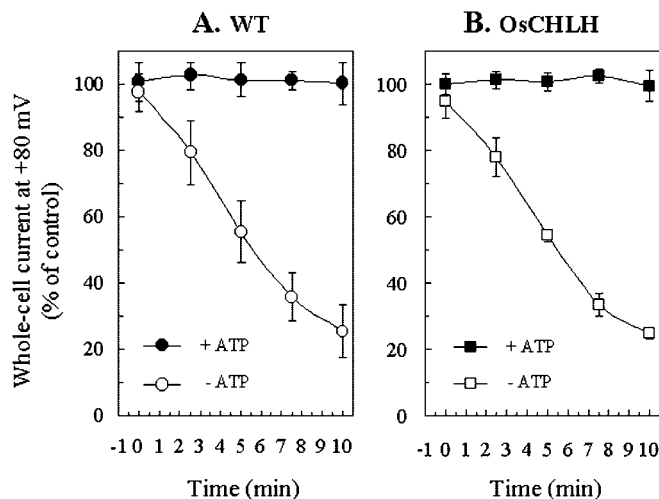


FIG. 7. Time course of whole cell currents at +80 mV in rice mesophyll protoplasts of wild type and mutant plants. The channel currents were measured immediately after gaining access to whole cells (within 20 s) in the presence or absence of 2 mM ATP in the pipette solution. Whole cell current magnitude at +80 mV, (relative to control current at that voltage) is shown. Data are presented as the average \pm S.E. of mesophyll cells ($n = 6$ for wild type, $n = 8$ for mutant). The voltage steps ranged between -160 and +100 mV in 20-mV increments from a holding potential of -40 mV. A, wild type; B, mutant. +ATP and -ATP indicate the presence and absence of ATP in the pipette solution, respectively. Other experimental conditions are as described in the legend to Fig. 5.

channel activities declined in a time-dependent manner. K_{out} channel activity at 10 min was only 25% of initial levels and showed the potential of half-activation ($V_{1/2}$) at ~ 5.5 min in both wild type and mutant cells. In addition, oligomycin signif-

icantly reduced the activity of the K_{out} channel in mutant cells (13.2% less than wild type) (data not shown). These results suggest that the cytosolic ATP originated from mitochondria-activated ATP-dependent K_{out} channels.

DISCUSSION

In animal cells there is good evidence that mitochondria are the predominant source of ATP (5–13). In plants, biomass production is ultimately determined by the ratio between photosynthesis and mitochondrial respiration (59). These metabolic pathways produce redox equivalents and ATP to meet the cellular energy requirements for growth and maintenance (2). However, in plants it remains unclear to what extent mitochondria contribute to cytosolic ATP levels.

To address this question, we investigated the activities of ATP-dependent K_{out} channels in mesophyll cells from seedlings of the *OsCHLH* rice mutant. The chloroplasts of the *OsCHLH* rice mutant lack the largest subunit of Mg^{2+} -chelatase, which is a key enzyme in the chlorophyll branch of the tetrapyrrole biosynthetic pathway (1). The mutant plants exhibited no chlorophyll fluorescence in intact leaves or in mesophyll cells, indicating that *OsCHLH* rice mutant plants lacked photosynthetic capacity (Fig. 1). This was further supported by measurements of photosynthetic activity (CO_2 gas exchange (Fig. 2) and O_2 evolution (Fig. 3)). Light-induced growth of the mutant was ~50% of that observed in wild type plants (data not shown). Despite impaired photosynthesis and slower growth, the light-grown *OsCHLH* rice mutant seedlings were well developed with fully expanded leaves, indicating that growth can occur in the absence of photosynthesis (20, 30). It is likely that the cytochrome and its branched alternative respiratory pathways in mitochondria coordinately balance ubiquinone pool oxidation/reduction and carbon skeleton turnover in response to cytosolic ATP levels (60). Sucrose enhanced the growth of the wild type and mutant seedlings, although the growth of the mutant in the presence of sucrose was still only 58.2% of that of wild type (data not shown). Sucrose-induced increases in growth were most likely because of enhanced metabolic pathways that produced redox equivalents and ATP via the activation of mitochondria functions.

Mitochondrial functions of the *OsCHLH* mutant were similar to those of the wild type, as determined by measuring O_2 concentrations in intact leaves (Fig. 3B). No statistically significant differences in O_2 consumption were observed in dark respiration. On the other hand, the *OsCHLH* mutant plants released higher levels of CO_2 during dark respiration, indicating that mitochondrial activity of the *OsCHLH* mutant was 62.5% higher than that of wild type (Fig. 2B). This quantitative difference between O_2 uptake and CO_2 release of the *OsCHLH* mutant plants in the dark seems to depend on the plant age and/or the experimental conditions. Photosynthetic O_2 evolution was modest (10–15% when it was normalized at $900 \mu\text{mol m}^{-2} \text{s}^{-1}$) in wild type seedlings at a low irradiance of $60 \mu\text{mol m}^{-2} \text{s}^{-1}$ and robust ($\sim 4 \mu\text{mol min}^{-1} \text{g}^{-1}$ fresh weight) at a saturating light pulse of $900 \mu\text{mol m}^{-2} \text{s}^{-1}$. In contrast, no photosynthetic O_2 evolution was observed in the *OsCHLH* mutant seedlings, even under saturating light conditions. We believe that the observation of O_2 consumption in the dark with the same blank (control) is artifactual and is caused by the 3-min light pulse. Although we used heat filtration this is because the rate of oxygen diffusion to the detector is temperature limited in a closed system. The absence of O_2 evolution in the *OsCHLH* mutant plants is attributable to the lack of chlorophyll (Fig. 1) and CP43 immunoreactivity (data not shown) in the thylakoid membranes. The CP43 subunit of PS II functions in light harvesting, and the absence of CP43 expression is

consistent with the lack of photosynthetic activity in these plants.

Interestingly, the *OsCHLH* mutant still exhibited mitochondrial-mediated CO_2 release (Fig. 2B) as well as O_2 consumption (Fig. 3B) in the light that progressively decreased. These results are consistent with light-induced inhibition of mitochondrial respiration, which has been reviewed previously (2). Light regulation of mitochondrial ATP production was also observed in the mutant seedlings as evidenced by a dramatic reduction of ATP levels (Fig. 4A) as O_2 consumption is closely coupled to mitochondrial ATP synthesis (2, 48). However, the decrease of ATP levels in the light is not because of CO_2 assimilation in the *OsCHLH* mutant as in the mutant light did not induce CO_2 uptake as it did in the wild type (compare traces in Fig. 2A). It is important to note that the decrease in O_2 consumption that we measured in the mutant resulted from light-induced inhibition of mitochondrial respiration. The rates of net O_2 uptake, which are nearly identical to net CO_2 release, are comprised of O_2 evolution in the Hill reaction of PS II, O_2 consumption by the Mehler reaction and the glycolytic pathway, and O_2 consumption in mitochondrial respiration in the light, whereas photorespiratory CO_2 evolution is accompanied by CO_2 uptake in the Calvin cycle and CO_2 release from mitochondrial respiration (61). Based on these facts and the photosynthetic properties of the *OsCHLH* mutant it is possible that respiration in the light may depend on the amount of photosynthetic primary products (61, 62), which the mutants are expected to lack because there is no photosynthetic CO_2 fixation. This could explain, as it does in drought-stressed plants (61) the substantial decrease of mitochondrial O_2 uptake and CO_2 release in the *OsCHLH* mutant in the light. This has been well established in both animal and plant cells, emphasizing that inhibition of ATP synthesis by light occurs in mitochondria (2, 64, 65). However, light markedly stimulates ATP synthesis via oxidative phosphorylation and O_2 uptake in photosynthetic cells (3, 4, 67), tobacco (68), wheat (64, 69), and barley mitochondria (70). A large body of evidence suggests that mitochondria are involved in photosynthetic metabolism, particularly with respect to ATP production (2). The level of ATP increased by 11–26% after exposure to light (71). In this case, the cytochrome and alternative pathways of mitochondrial electron transport might be involved in such reactions. How are the contradictory findings in the literature concerning mitochondrial respiration in light to be explained? Further studies in the regulation of mitochondrial activity during photosynthesis are needed. Our data revealed that the *OsCHLH* rice mutant plants have similar levels of mitochondrial activity as the wild type but lack photosynthetic capacity. The mutant plants provide ATP to meet the cellular energy requirements for growth and maintenance solely from mitochondrial functions.

During oxidation of the redox equivalents in the mitochondrial respiratory electron transport chain, O_2 is consumed and a proton gradient is formed across the inner mitochondrial membrane. This proton gradient provides energy for ATP synthesis in the mitochondria, a process termed oxidative phosphorylation. ATP production in darkness was similar in wild type and mutant cells (Fig. 4B), which is consistent with similar rates of O_2 uptake (Fig. 3B). Oligomycin ($2 \mu\text{g ml}^{-1}$), which is known to inhibit mitochondrial H^+ -ATP synthase (72), significantly inhibited the level of cytosolic ATP in both wild type and mutant cells, effectively inhibiting mitochondrial respiration. DCMU also inhibited ATP production in both wild type and mutant cells, although *OsCHLH* plants lack photosynthetic capacity. This appears to be because of the inhibition of cytochrome *b* oxidation-reduction by DCMU at one ubiquinone site, presumably ubiquinone (Q1) redox near the inner side of

the mitochondrial membrane (48). The combined inhibitory effects of oligomycin and DCMU on ATP production were synergistic although the binding sites for the two compounds were specific.

In the presence of glucose as a substrate, oxidative phosphorylation was 154 and 152% of control levels, for wild type and mutant cells, respectively. Oligomycin reduced ATP levels by 66 and 70% in wild type and mutant cells, whereas it showed a much greater effect in the absence of glucose, decreasing ATP levels by ~75% in both cell types. Iodoacetic acid inhibited ATP production by 36% in both wild type and mutant cells. Taken together, these findings suggest that glycolysis is functional in both wild type and mutant cells. However, glycolysis, which is the initial stage of glucose metabolism, produces a relatively small amount of ATP in plant cells (Fig. 4B). Therefore, oxidative phosphorylation represents the primary source of ATP in the chlorophyll-deficient *OsCHLH* rice mutant. These cells are capable of maintaining a steady-state flux of energy from mitochondrial oxidative phosphorylation, which provides ATP for the cytosolic ATPases to perform essential cellular functions.

K⁺ is the most abundant cation in the cytoplasm of living cells, and it regulates ionic strength, osmotic potential, and membrane polarization. Permeability to K⁺ is mediated by voltage-dependent K⁺ channels, which are by far the best characterized plasma membrane ion channels in plant cells (73). It has been established in a variety of cell types that activation of K_{out} channels under steady-state conditions is dependent on cytoplasmic ATP, and a lack of ATP causes channel "run-down" (16, 17, 19, 24, 54–58). The activation of various protein kinases, PP1, PP2A, and PP2C are required for the up-regulation of K_{out} channel currents in *Samanea*, *Tobacco*, and *Vicia* mesophyll cells (51, 56, 74). Our data show that *rice* mesophyll cells also exhibit voltage-dependent K⁺ current and that ATP is required for its activation (Figs. 5–7). The magnitude of current in wild type cells was greater in the presence of ATP than that of mutant (Fig. 6). The smaller whole cell current in the mutant cells might be because of a combination of environmental conditions and epistatic interactions, which are the two main factors controlling the effects of deleterious mutations (63). One could therefore expect that the number of K⁺ channels in the plasma membrane is different in the wild type and mutant cells because the mutant seedlings were poorly developed (Fig. 1A), although the mitochondrial respiratory activity is quite similar to that of wild type (Figs. 3B and 4B). Interestingly, rice mesophyll cells lacked the inward K⁺ current that is found in guard cells (16, 19, 26, 42, 49, 50, 52, 66). The ATP-activated K_{out} channel current was maintained over periods of 10 min from the beginning of patch recording in both wild type and mutant cells.

We also found that the ATP-dependent K_{out} channel current was largely inhibited by oligomycin, which blocks mitochondrial F₁F₀-ATPase, in both wild type and mutant cells (data not shown). These data further supported the idea that a cytosolic ATP pool derived from mitochondria maintained the activation of the K_{out} channel current in mutant cells. However, a previous study suggested that activation of K⁺ channels, including K_{out} and non-selective cation channels, was mediated by ATP produced photosynthetically from albino mutant (*alb-1*) plant cells (16). Thus, the role of mitochondria in the stimulation of the K_{out} channel current remains controversial. More recent studies showed that light-induced membrane hyperpolarization is modulated by photosynthesis-dependent plasma membrane H⁺-ATPases in mesophyll cells (27, 29). However, this hyperpolarization clearly occurred in response to light absorption by pigments other than chlorophyll, demonstrating that chlorophyll-deficient cells also exhibit light-induced membrane

hyperpolarization (30), which differs from the findings of the earlier study (16). Taken together, the data suggest that light-driven photosynthesis is not directly involved in the activation of K_{out} channel current in the plasma membrane, although the possibility of direct K⁺ transport by other ATPases (*i.e.* K⁺-ATPases) cannot be ruled out (17). Mitochondrial respiration therefore provides the source of cytosolic ATP. From these results, we strongly suggest that mitochondria in the *OsCHLH* mutant plays a major role in meeting the cytosolic energy requirements during plant growth and development.

Acknowledgements—C.-H. Goh thanks members of the Hetherington laboratory for advice and support on the patch clamp experiments and also acknowledges Dr. W. S. (Fred) Chow, The Australian National University, for helpful discussions on the O₂ evolution experiments and for critically reading the manuscript.

REFERENCES

- Jung, K.-H., Hur, J., Ryu, C.-H., Choi, Y., Chung, Y.-Y., Miyao, A., Hirochika, H., and An, G. (2003) *Plant Cell Physiol.* **44**, 463–472
- Krömer, S. (1995) *Annu. Rev. Plant Physiol. Plant Mol. Biol.* **46**, 45–70
- Padmasree, K., Padmavathi, L., and Raghavendra, A. S. (2002) *Crit. Rev. Biochem. Mol. Biol.* **37**, 71–119
- Gardestrom, P., and Lernmark, U. (1995) *J. Bioenerg. Biomembr.* **27**, 415–421
- Buttgereit, F., and Brand, M. D. (1995) *Biochem. J.* **312**, 163–167
- Brown, G. C., Lakin-Thomas, P. L., and Brand, M. D. (1990) *Eur. J. Biochem.* **192**, 355–362
- Larsson, N., and Clayton, D. (1995) *Annu. Rev. Genet.* **29**, 151–178
- Smeitink, J., van Den Heuvel, L., and Dimauro, S. (2001) *Nat. Rev. Genet.* **2**, 342–352
- Norma, A. (1983) *Nature* **305**, 147–148
- Rorsman, P., and Trube, G. (1990) in *Potassium Channels. Structure, Classification, Function and Therapeutic Potential* (Cook, N. S., ed) pp. 96–116, Halsted Press, New York
- Priebe, L., Friedrich, M., and Benndorf, K. (1996) *J. Physiol.* **492**, 405–417
- Knopp, A., Thierfelder, S., Doepner, B., and Benndorf, K. (2001) *Cardiovasc. Res.* **52**, 236–245
- Carrasco, A. J., Dzeja, P., Alekseev, A. E., Pucar, D., Zingman, L. V., Abraham, M. R., Hodgson, D., Bienengraeber, M., Puceat, M., Janssen, E., Wieringa, B., and Terzic, A. (2001) *Proc. Natl. Acad. Sci. U. S. A.* **19**, 7623–7628
- Weiss, J. N., and Lamp, S. T. (1989) *J. Gen. Physiol.* **94**, 911–935
- Weiss, J. N., and Hiltbrand, B. (1985) *J. Clin. Invest.* **75**, 436–447
- Spalding, E. P., and Goldsmith, M. (1993) *Plant Cell* **5**, 477–484
- Briskin, D. P., and Gawienowski, M. C. (1996) *Plant Physiol.* **111**, 1199–1207
- Moran, N. (1996) *Plant Physiol.* **111**, 1281–1292
- Keunecke, M., and Hansen, U. P. (2000) *Planta* **210**, 792–800
- Van Volkenburgh, E., and Cleland, R. E. (1990) *Planta* **182**, 72–76
- Taylor, A. R., and Assmann, S. M. (2001) *Plant Physiol.* **125**, 329–338
- Goh, C.-H., Oku, T., and Shimazaki, K. (1995) *Plant Physiol.* **109**, 187–194
- Goh, C.-H., Kinoshita, T., Oku, T., and Shimazaki, K. (1996) *Plant Physiol.* **111**, 433–440
- Romano, L. A., Miedema, H., and Assmann, S. M. (1998) *Plant Cell Physiol.* **39**, 1133–1144
- Spalding, E. P. (2000) *Plant Cell Environ.* **23**, 665–674
- Goh, C.-H., Dietrich, P., Steinmeyer, R., Schroeder, U., Nam, H.-G., and Hedrich, R. (2002) *Plant J.* **32**, 623–630
- Stiles, K. A., and Van Volkenburgh, E. (2002) *J. Exp. Bot.* **53**, 1651–1657
- Stahlberg, R., and Van Volkenburgh, E. (1999) *Planta* **208**, 188–195
- Harada, A., Okazaki, Y., and Tagaki, S. (2002) *Planta* **214**, 863–869
- Stahlberg, R., Van Volkenburgh, E., and Cleland, R. E. (2000) *Planta* **212**, 1–8
- Spalding, E. P., Slayman, C. L., Goldsmith, M. H. M., Gradmann, D., and Bertl, A. (1992) *Plant Physiol.* **99**, 96–102
- Assmann, S. M., Simoncini, L., and Schroeder, J. I. (1985) *Nature* **318**, 285–287
- Vanselow, K. H., and Hansen, U.-P. (1989) *J. Membr. Biol.* **110**, 175–187
- Krömer, S., Malmberg, G., and Gardestrom, P. (1993) *Plant Physiol.* **102**, 947–955
- Dutilleul, C., Garmier, M., Noctor, G., Mathieu, C., Chétrit, P., Foyer, C. H., and de Paepe, R. (2003) *Plant Cell* **15**, 1212–1226
- Goh, C.-H., Schreiber, U., and Hedrich, R. (1999) *Plant Cell Environ.* **22**, 1057–1070
- Jeong, W. J., Park, Y.-I., Suh, K., Raven, J. A., Yoo, O. J., and Liu, J. R. (2002) *Plant Physiol.* **129**, 112–121
- Choi, S. M., Jeong, S. W., Jeong, W. J., Kwon, S. Y., Chow, W. S., and Park, Y. I. (2002) *Planta* **216**, 315–324
- Walker, D. (1987) *The Use of the Oxygen Electrode and Fluorescence Probes in Simple Measurements of Photosynthesis*, Oxygraphics, Sheffield, UK
- Manfredi, G., Yang, L., Gajewski, C. D., and Mattiazzi, M. (2002) *Methods* **26**, 317–326
- Bradford, M. M. (1976) *Anal. Biochem.* **72**, 248–254
- Li, W., and Assmann, S. M. (1993) *Proc. Natl. Acad. Sci. U. S. A.* **90**, 262–266
- Neher, E. (1992) *Methods Enzymol.* **207**, 123–131
- Jensen, P. E., Willows, R. D., Petersen, B. L., Vothknecht, U. C., Stummann, B. M., Kannangara, C. G., von Wettstein, D., and Henningsen, K. W. (1996) *Mol. Gen. Genet.* **250**, 383–394
- Bricker, T. M., Young, A., Frankel, L. K., and Putnam-Evans, C. (2002) *Biochim. Biophys. Acta* **1556**, 92–96
- Rosenberg, C., Christian, J., Bricker, T. M., and Putnam-Evans, C. (1999)

- Biochemistry* **38**, 15994–16000
47. Xie, Z., and Chen, Z. (1999) *Plant Physiol.* **120**, 217–225
48. di Rago, J. P., and Colson, A. M. (1988) *J. Biol. Chem.* **263**, 12564–12570
49. Bei, Q., and Luan, S. (1998) *Plant J.* **13**, 857–865
50. Kourie, J., and Goldsmith, M. H. M. (1992) *Plant Physiol.* **98**, 1087–1097
51. Li, W., Luan, S., Schreiber, S. L., and Assmann, S. M. (1994) *Plant Physiol.* **106**, 957–961
52. Bert, A., Anderson, J. A., Slayman, C. L., and Gaber, R. F. (1995) *Proc. Natl. Acad. Sci. U. S. A.* **92**, 2701–2705
53. Homann, U., and Thiel, G. (2002) *Proc. Natl. Acad. Sci. U. S. A.* **99**, 10215–10220
54. Zimmermann, S., Thomin, S., Guern, J., and Barbier-Brygoo, H. (1994) *Plant J.* **6**, 707–716
55. Davies, J. M., and Sander, D. (1995) *J. Membr. Biol.* **145**, 75–86
56. Thomin, S., Zimmermann, S., Guern, J., and Barbier-Brygoo, H. (1995) *Plant Cell* **7**, 2091–2100
57. Leonhardt, N., Marin E., Vavasseur, A., and Forestier, C. (1997) *Proc. Natl. Acad. Sci. U. S. A.* **94**, 14156–14161
58. Trapp, S., Tucker, S. J., and Ashcroft, F. M. (1998) *J. Gen. Physiol.* **112**, 325–332
59. Lambers, H. (1997) in *Oxidation of Mitochondrial NADH and the Synthesis of ATP* (Dennis, D. H., Turpin, D. H., Lefebvre, D. D., and Layzell, D. B., eds) pp. 200–219, Addison Wesley Longman, Harlow Press, London, UK
60. Vanlerberghe, G. C., and McIntosh, L. (1997) *Annu. Rev. Plant Physiol. Plant Mol. Biol.* **48**, 703–734
61. Pärnik, T., and Keerber, O. (1995) *J. Exp. Bot.* **46**, 1439–1447
62. Haupt-Herting, S. Klug, K., and Fock, H. P. (2001) *Plant Physiol.* **126**, 388–396
63. Kishony, R., and Leibler, S. (2003) *J. Biol.* <http://jbiol.com/content/2/2/14>
64. Pastore, D., Di Martino, C., Bosco, G., and Passarella, S. (1996) *Biochem. Mol. Biol. Int.* **39**, 149–157
65. Vekshin, N. L. (1991) *Biochem. Int.* **25**, 603–611
66. Pineros, M. A., and Kochian, L. V. (2003) *Plant Physiol.* **131**, 583–594
67. Raghavendra, A. S., Padmasree, K., and Saradedevi, K. (1994) *Plant Sci.* **97**, 1–14
68. Rey, P., and Peltier, G. (1989) *Plant Physiol.* **89**, 762–767
69. Stitt, M., and Lilley, R. M. (1982) *Plant Physiol.* **70**, 971–977
70. Gardeström, P. (1987) *FEBS Lett.* **212**, 114–118
71. Spalding, E. P., and Cosgrove, D. J. (1992) *Plant Physiol.* **188**, 199–205
72. Valerio, M., Diolet, P., and Haraux, F. (1993) *Eur. J. Biochem.* **216**, 565–571
73. Maathuis, F. J., Ichida, A. M., Sanders, D., and Schroeder, J. I. (1997) *Plant Physiol.* **114**, 1141–1149
74. Cohen, P. (1992) *Trends Biochem. Sci.* **17**, 408–413